Interrogating vertically oriented carbon nanofibers with nanomanipulation for nanoelectromechanical switching applications

Anupama B. Kaul,[1,a] Abdur R. Khan,[1,2] Leif Bagge,[1,3] Krikor G. Megerian,[1] Henry G. LeDuc,[1] and Larry Epp[1]
[1]*Jet Propulsion Laboratory, California Institute of Technology, Pasadena, California 91109, USA*
[2]*Keck School of Medicine, University of Southern California, Los Angeles, California 90089, USA*
[3]*Department of Electrical and Computer Engineering, University of Texas, Austin, Texas 78712, USA*

(Received 22 June 2009; accepted 31 July 2009; published online 31 August 2009)

We have demonstrated electrostatic switching in vertically oriented carbon nanofibers synthesized on refractory metallic nitride substrates, where pull-in voltages V_{pi} ranged from 10 to 40 V. A nanoprobe was used as the actuating electrode inside a scanning-electron microscope and van der Waals interactions at these length scales appeared significant, suggesting such structures are promising for nonvolatile memory applications. A finite element model was also developed to determine a theoretical V_{pi} and results were compared to experiment. Nanomanipulation tests also revealed tubes synthesized directly on Si by dc plasma-enhanced chemical-vapor deposition with ammonia and acetylene were electrically unsuitable for dc nanoelectromechanical switching applications. © *2009 American Institute of Physics*. [DOI: 10.1063/1.3211851]

Performance limitations of Si integrated circuits as a result of continued miniaturization[1] has created an ever-increasing need for exploring materials and architectures beyond solid-state transistors. Nanoelectromechanical (NEM) switches may overcome these limitations, by reducing leakage currents and power dissipation. They also provide the potential for enhanced radiation tolerance and high temperature resilience. The exceptional mechanical elasticity of carbon nanotubes (CNTs) also suggests such materials are well-suited for NEM switching applications for increased cycling longevity, when compared to inorganic materials such as semiconducting[2] or metallic nanowires.[3]

Nanotube-based NEM switches have already been demonstrated for a variety of applications,[4–6] where the tubes were oriented parallel to the substrate. Here, we consider tubes perpendicular to the substrate, which is an architecture that lends itself to increased integration density for three-dimensional (3D) electronics. Switching between vertically oriented tubes arranged in a three-terminal configuration was recently reported by Jang *et al.*[7] In this paper, we demonstrate electrostatic switching in vertically oriented tubes or carbon nanofibers (CNFs) synthesized using dc plasma-enhanced (PE) chemical-vapor deposition (CVD), where a nanoprobe inside a scanning electron microscope (SEM) was used to actuate single tubes. PECVD synthesized tubes are attractive for device applications due to their more controlled alignment. Nanomanipulation was also used to interrogate the electrical conduction in individual, as-grown CNFs on Si, as well as on refractory nitride underlayers. Finally, finite-element modeling (FEM) was used to determine the pull-in voltage V_{pi} theoretically, and results were compared to experiment.

Individual CNFs were formed by first patterning Ni catalyst islands using e-beam evaporation and lift-off. The CNFs were then synthesized using dc PECVD with C_2H_2:NH_3 =[1:4] at 5 Torr and 700 °C.[8] Tubes were grown directly on Si ⟨100⟩ substrates with resistivity $\rho \sim 1-5$ mΩ cm, and NbTiN. The ~200 nm thick refractory NbTiN was sputtered,[9] with $\rho \sim 113$ μΩ cm, and was also found to be chemically compatible with CNF synthesis. The sample was mounted on a 45° beveled holder inside the SEM (thus all SEMs reported are at a 45° tilt angle). A nanomanipulator probe stage (Kammrath and Weiss) was placed inside the SEM (FEI Quanta 200F), where tungsten probes were used to make *in situ* electrical measurements with an HP 4155C parameter analyzer.

The nanoprobe physically contacted an individual CNF grown on NbTiN, as shown by the SEM in the inset of Fig. 1(a) (ground probe was on substrate). Since the probe-to-tube contact length was <100 nm for this two-terminal measurement, conduction was dominated by the large contact resistance. The work function φ for tungsten (W) $\varphi_W \sim 4.5$ eV $< \varphi_{CNF} \sim 5.0$ eV,[10] and suggests a Schottky barrier may arise at this interface, and also possibly at the tube-to-substrate interface; $\varphi_{NbN} \sim 3.92$ eV and like most transition metal nitrides with low φ,[11] it is likely $\varphi_{NbTiN} < \varphi_{CNF}$. A subgap region with suppressed conductance at low biases was seen in both polarities, and may have arisen from a

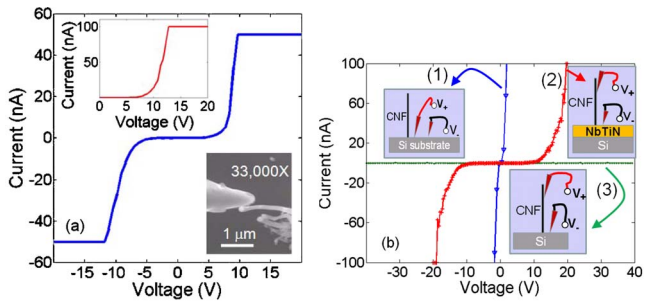

FIG. 1. (Color online) (a) Electrical continuity measurements for a single CNF grown on NbTiN. A nanoprobe is in contact with CNF, as indicated by the SEM image. The inset shows compliance increased to 100 nA. (b) Curve (1) corresponds to the case where both probes were shorted to the substrate with high conductivity; curve (2) showed the tube on NbTiN is electrically conductive; curve (3) corresponds to the case where no transport could be detected for a tube grown on Si, and suggests such tubes are unsuitable for dc NEMS applications.

[a]Electronic mail: anupama.b.kaul@jpl.nasa.gov. Tel.: (818) 393-7186.

native oxide on the W probes; if a small semiconducting junction (e.g., Schottky) also exists, an asymmetry in the *I-V* characteristic would arise, as observed.

The currents measured are likely to propagate via the tube surface or sidewalls which is necessary for the application of CNFs in dc NEMS. This is illustrated in the following measurements [Fig. 1(b)] performed on tubes grown directly on Si, as well as on NbTiN under layers. Curve (1) in Fig. 1(b) indicated high conductivity as expected since both probes were shorted to the substrate. When a tube grown on NbTiN was probed [curve (2)], a response similar to Fig. 1(a) was detected. However, no measurable currents for the tube grown directly on Si were observed [curve (3)], which could arise from a dielectric coating (e.g., SiN_x) on the sidewalls due to Si resputtering and reacting with the nitrogen rich gaseous environment (~80% NH_3).[12] Any SiN_x on the substrate is likely to be removed due to the directional nature of ions bombarding the substrate. Since sidewall conduction is of little interest for field emission application of such tubes,[13] where transport occurs primarily through the electrically conducting tube body, nanomanipulation measurements performed here uniquely suggest tubes synthesized directly on Si are unsuitable for dc NEMs applications. In the case of tubes on NbTiN, although more nitrogen rich phases could be present, an electrically insulating sheath on the tube sidewalls was not evident.

Actuation measurements were performed for CNFs on NbTiN, where a nanoprobe was manipulated to within a few hundred nanometers of a single CNF. The electrostatic force per unit length F_{elec} increases as $F_{elec} < V^2$, where V is the voltage, and the elastostatic force per unit length F_{elasto} increases as $F_{elasto} < EI$, where E and I are the elastic modulus and moment of inertia of the nanotube, respectively.[14] With increasing V ($F_{elec} > F_{elasto}$) the tube deflects closer to the probe, and a tunneling current is detected which increases exponentially, and results in a sudden or sharp change in slope at turn-on. The switching *I-V* in Fig. 2(a) shows currents rising sharply at $V_{pi} \sim 18$ V. The turn-off occurred at ~16 V and was dominated by the large tube-to-probe contact resistance since the tube remained stuck to the probe; thus, the turn-off response was similar to Fig. 1(a). The inset in Fig. 2(a) captures another switching event for a different tube, where turn-on and turn-off occurred at ~14 and 10 V, respectively, and also illustrates the abruptness of the turn-on transition.

In Fig. 2(b), the SEM image in the top inset shows a different tube just prior to actuation with a tube length $l \sim 2.8$ μm, initial gap $g_0 \sim 160$ nm, tube diameter $d \sim 60$ nm, and a probe-to-tube coupling length $c \sim 0.63$ μm. The bottom inset shows the tube stuck to the probe after actuation. From Fig. 2(b), in the regime where the current rises from a nonzero to a maximal value (between 26–31 V), the data appears to be increasingly noisy which can be attributed to the stochastic nature of the tunneling mechanism. Surface asperities on the W probes may also lead to random fluctuations in the current during the switching process. The SEM image in the bottom inset suggests that the van der Waals force $F_{vdw} > F_{elasto}$ which is validated by the hysteresis in the *I-V* of Fig. 2. While Jang *et al.*[7] also reported stiction for vertically oriented tubes, no hysteresis data was presented that electrically signaled the presence of stiction, as has been reported here.

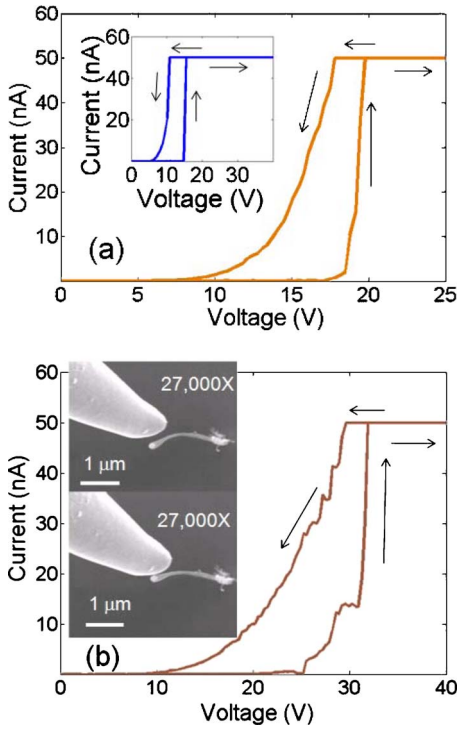

FIG. 2. (Color online) (a) Actuation test where a nanoprobe was within hundred's of nm of a CNF. Turn-on and turn-off were at ~18 V and 16 V, respectively, where turn-off was dominated by the tube-to-probe contact resistance. The inset shows another tube where turn-on and turn-off occurred at ~14 and 10 V, respectively, and also indicates the abruptness of the turn-on transition. (b) SEM image in the top inset for a tube just prior to actuation, with $l \sim 2.8$ μm, $g_0 \sim 160$ nm, $d \sim 60$ nm, and $c \sim 0.63$ μm; bottom inset depicts the tube stuck to the probe after actuation. The *I-V* characteristic for switching showed $V_{pi} \sim 31$ V. Hysteresis in the *I-V* suggests such structures are promising for nonvolatile memory applications.

The top SEM image in the inset of Fig. 3(a) shows the same tube but with larger $g_0 \sim 220$ nm just before actuation, while the bottom SEM shows the tube just after actuation. A larger g_0 should increase V_{pi}, which was seen in the *I-V* of Fig. 3(a), where the onset of a current occurs at ~32 V (cycle 1). Although the bottom SEM image in the inset of Fig. 3(a) shows the tube stuck to the probe after actuation, with a contact length <50 nm, it detached prior to the onset of cycle 2. In cycle 2, $V_{pi} \sim 35$ V, but the turn-off was almost identical to cycle 1, since it was dominated by the

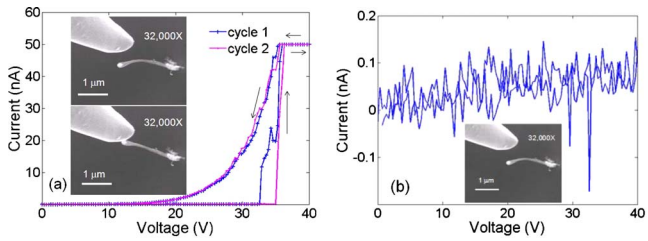

FIG. 3. (Color online) (a) The top SEM in the inset shows $g_0 \sim 220$ nm for the same CNF in Fig. 2(b) just before actuation. The bottom SEM in the inset shows the tube after actuation, where it was momentarily stuck to the probe, but detached prior to the onset of cycle 2. The *I-V* shows 2 switching cycles with turn-on varying slightly (~32 and 35 V) but very little variation was seen in the turn-off cycles. (b) The gap was increased further to >400 nm, as shown by the SEM in the inset, where the *I-V* indicates the absence of switching and confirms the scaling of V_{pi} with g_0, to first order. From this, leakage currents in the instrumentation were <150 pA (peak-to-peak) up to 40 V.

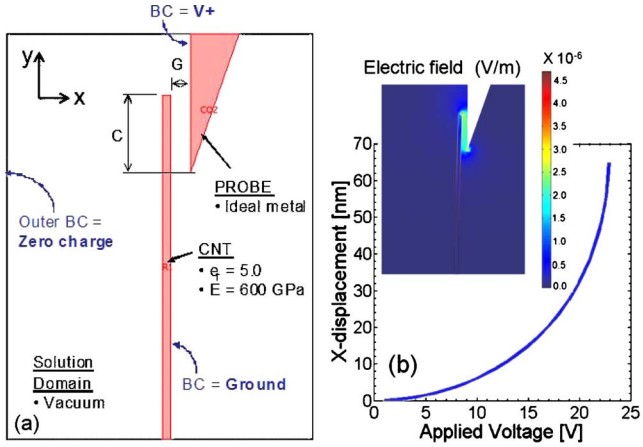

FIG. 4. (Color online) (a) Geometry and boundary conditions used in the FEM simulations. (b) The nanotube tip displacement x as a function of V, where E=600 GPa, l=2.8 μm, g_0=160 nm, d=60 nm, c=630 nm [parameters from Fig. 2(b)]. Inset showed the spatial profile of the electric field strength at ~22.9 V, just prior to pull-in, and indicates the field is distributed between the nanoprobe and CNF. The V_{pi}(numerical)~23 V and V_{pi}(experiment)~31 V for this geometry.

contact resistance. When g_0 was increased to >400 nm [SEM image in the inset of Fig. 3(b)], a switching event could not be detected, confirming the scaling trend of V_{pi} with g_0, to first order. From the I-V in Fig. 3(b), we also deduce very low leakage currents in the instrumentation (<150 pA peak-to-peak up to 40 V).

The V_{pi}(analytical) was calculated using V_{PI}(analytical) $=\sqrt{(8kg_0^3)/(27\varepsilon_o wl)}$, where ε_o is the effective permittivity, and w is the beam width (or tube diameter). The spring constant k for a cantilever beam (our tubes are akin to a vertical cantilever) is given by $k=(8EI)/l^3$. A V_{pi}(analytical)~13 V was computed for the geometry in Fig. 2(b), which assumed the probe and tube couple over l entirely. FEM with COMSOL MULTIPHYSICS[15] was used to determine V_{pi}(numerical) since the probe interacts with the tube predominately near the tip. Figure 4(a) illustrates the two-dimensional model with the boundary conditions (E_{CNF} ~600 GPa).[16] The V_{pi}(numerical)~23 V>V_{pi}(analytical) ~13 V confirming expectations since COMSOL accounts for the smaller coupling area between the probe and the tube. The F_{elec} and F_{elasto} were calculated by numerically solving the Poisson's equation and the strain tensor, respectively, to determine the equilibrium position of the tube by a force balance analysis. Since electrostatic actuation is a positive feedback effect, an instability arises at a critical gap g_c, where no equilibrium solution exists, and the tube collapses to the probe at this pull-in point. In the tube deflection-voltage characteristic of Fig. 4(b) $(\partial x)/(\partial V)|_{V=V_{pi}} \rightarrow \infty$ occurs at $x=g_c$~61 nm, and V_{pi}(numerical)~23 V. With g_0 ~160 nm, g_c/g_o=61 nm/160 nm~0.38, which is in close agreement with the value obtained in microelectromechanical switches ($g_c \sim g_0/3$), as well as continuum simulations on other CNT structures,[14] where g_c/g_o~0.4 (e.g., Fig. 10 of Ref. 14). The V_{pi}(experiment) was ~31 V [Fig. 2(b)] and the 8 V discrepancy could arise from the assumption that the tube had a uniform d and was perfectly straight, which was not the case empirically, and E may have been >600 GPa on this tube.

In conclusion, we have experimentally demonstrated electrostatic switching in vertically oriented PECVD grown nanotubes on NbTiN substrates, where the hysteresis data presented suggests that such structures are promising for 3D nonvolatile memory applications.

We acknowledge assistance from R. Ruiz, and G. DeRose and B. Chim both of the California Institute of Technology (Caltech), with SEM setup, R. Kowalczyk for assistance with PECVD, and P. von Allmen and R. Baron for useful discussions. We gratefully acknowledge critical support and infrastructure provided for this work by the Kavli Nanoscience Institute at Caltech. This research was carried out at the Jet Propulsion Laboratory, California Institute of Technology, under a contract with the National Aeronautics and Space Administration and was funded through the internal Research and Technology Development (R&TD) program (01STCR, R.08.023.060).

[1] International Technology Roadmap for Semiconductors, http://www.itrs.net/Links/2008ITRS/Update/2008_Update.pdf.
[2] H. T. Ng, J. Li, M. K. Smith, P. Nguyen, A. Cassell, J. Han, and M. Meyyappan, Science **300**, 1249 (2003).
[3] A. Husain, J. Hone, H. W. Ch. Postma, X. M. H. Huang, T. Drake, M. Barbic, A. Scherer, and M. L. Roukes, Appl. Phys. Lett. **83**, 1240 (2003).
[4] T. Rueckes, K. Kim, E. Joselevich, G. Y. Tseng, C. L. Cheung, and C. M. Lieber, Science **289**, 94 (2000).
[5] E. Dujardin, V. Derycke, M. F. Goffman, R. Lefèvre, and J. P. Bourgoin, Appl. Phys. Lett. **87**, 193107 (2005).
[6] A. Eriksson, S. Lee, A. Sourab, A. Issacsson, R. Kaunisto, J. M. Kinaret, and E. E. B. Campbell, Nano Lett. **8**, 1224 (2008).
[7] J. E. Jang, S. N. Cha, Y. Choi, G. A. J. Amaratunga, D. J. Kang, D. G. Hasko, J. E. Jung, and J. M. Kim, Appl. Phys. Lett. **87**, 163114 (2005).
[8] K. B. K. Teo, M. Chhowalla, G. A. J. Amaratunga, W. I. Milne, G. Pirio, P. Legagneux, F. Wyczisk, J. Olivier, and D. Pribat, J. Vac. Sci. Technol. B **20**, 116 (2002).
[9] B. D. Jackson, G. de Lange, T. Zijlstra, M. Kroug, T. M. Klapwijk, and J. A. Stern, J. Appl. Phys. **97**, 113904 (2005).
[10] S. Ahmed, S. Das, M. K. Mitra, and K. K. Chattopadhyay, Appl. Surf. Sci. **254**, 610 (2007).
[11] Y. Saito, S. Kawata, H. Nakane, and H. Adachi, Appl. Surf. Sci. **146**, 177 (1999).
[12] A. V. Melechko, T. E. McKnight, D. K. Hensley, M. A. Guillorn, A. Y. Borisevich, V. I. Merkulov, D. H. Lowndes, and M. L. Simpson, Nanotechnology **14**, 1029 (2003).
[13] N. Shimoi and S. Tanaka, Carbon **47**, 1258 (2009).
[14] M. Dequesnes, S. V. Rotkin, and N. R. Aluru, Nanotechnology **13**, 120 (2002).
[15] COMSOL MULTIPHYSICS version, 3.4, COMSOL AB, Tegnérgatan 23, SE-111 40, Stockholm, Sweden. www.comsol.com.
[16] A. B. Kaul, P. Khan, A. T. Jennings, J. R. Greer, and P. von Allmen, "Electrostatic switching in vertically oriented nanotubes for nonvolatile memory applications," Mater. Res. Soc. Symp. Proc. (in press).